2003

Delta-ferrite recovery structures in low-carbon steels

Rian Dippenaar
University of Wollongong, rian@uow.edu.au

Dominic Phelan
University of Wollongong, phelan@uow.edu.au

Delta-ferrite recovery structures in low-carbon steels

Abstract

The development of delta-ferrite recovery substructures in low-carbon steels has been observed in-situ utilizing laser scanning confocal microscopy (LSCM). Well-developed sub-boundaries with interfacial energies much smaller than that of delta-ferrite grain boundaries formed following transformation from austenite to delta-ferrite on heating. It is proposed that transformation stresses associated with the austenite to delta-ferrite phase transformation generate dislocations that subsequently recover into sub-boundaries by a process of polygonization. Experimental evidence in support of this proposal was found in a ferritic stainless steel. Thermal cycling through the high-temperature delta-ferrite/austenite/delta-ferrite phase transformation leads to the development of a well-defined recovery substructure, which, in turn, modifies the low-temperature austenite decomposition product from Widmanstätten to polygonal ferrite, with a commensurate change in hardness.

Keywords

carbon, low, steels, structures, delta, ferrite, recovery

Disciplines

Engineering | Science and Technology Studies

Publication Details

Dippenaar, R. J. & Phelan, D. J. (2003). Delta-ferrite recovery structures in low-carbon steels. Metallurgical and Materials Transactions B: Process Metallurgy and Materials Processing Science, 34 (5), 495-501.

Delta-Ferrite Recovery Structures in Low-Carbon Steels

R.J. DIPPENAAR and D.J. PHELAN

The development of delta-ferrite recovery substructures in low-carbon steels has been observed *in-situ* utilizing laser scanning confocal microscopy (LSCM). Well-developed sub-boundaries with interfacial energies much smaller than that of delta-ferrite grain boundaries formed following transformation from austenite to delta-ferrite on heating. It is proposed that transformation stresses associated with the austenite to delta-ferrite phase transformation generate dislocations that subsequently recover into sub-boundaries by a process of polygonization. Experimental evidence in support of this proposal was found in a ferritic stainless steel. Thermal cycling through the high-temperature delta-ferrite/austenite/delta-ferrite phase transformation leads to the development of a well-defined recovery substructure, which, in turn, modifies the low-temperature austenite decomposition product from Widmanstätten to polygonal ferrite, with a commensurate change in hardness.

I. INTRODUCTION

ALTHOUGH it is generally conceded that the early stages of solidification and subsequent high-temperature phase transformations profoundly influence cast structure, conclusions have mostly been drawn from indirect experiments and very little work has been done on the direct observation of events. A fundamental understanding of the events occurring in the meniscus region of high-speed continuous casters, which determine the quality of the cast product, is of special interest. The delta-ferrite to austenite phase transformation occurs when the newly formed steel shell is relatively thin. The volume change and differences in thermal expansion of the phases may generate stresses, which, if the strength of this thin shell is exceeded, can lead to casting defects. Moreover, the delta-ferrite to austenite phase transformation may also play a role in the subsequent decomposition of austenite and, through this, the microstructural development on further cooling and, hence, the mechanical properties of the final product. The final alpha-ferrite grain size following decomposition from austenite in plain carbon steel is largely controlled by the grain size of the parent austenite because austenite grain boundaries, particularly grain corners, are the preferred sites for the nucleation of alpha ferrite.[1–4] A smaller austenite grain size will lead to refinement of the alpha ferrite grain size. In strip casting, and to a lesser extent in thin-slab casting, the opportunities for control of the microstructure through thermomechanical processing[5] are restricted. Therefore, the exact way in which the delta-ferrite to austenite phase transformation occurs following solidification becomes increasingly important.[6]

An impediment to success in previous studies has been the inability to study this high-temperature transformation directly because subsequent phase transformations mask the transformation mode. A second obstacle to a detailed study of delta-ferrite decomposition is the difficulty in obtaining sufficient resolution at the high temperatures pertaining to this phase transition; the emission of infrared light from a sample at such high temperatures renders the *in-situ* observation of events by optical microscopy very difficult.

The phase transformation from austenite to ferrite is accompanied by the generation of dislocations, which, through a subsequent process of recovery, can be rearranged into sub-boundaries, one such example being veining.[7] Hauser *et al.*[8] have shown that transformation stresses accompanying phase transformations can produce dislocation networks, even in the absence of mechanical work, in alpha ferrite and a number of other systems.[9,10] At elevated temperature, these dislocations can be reorganized into subgrain boundaries through a process of recovery, or more specifically polygonization. Hence, if austenite is heated into the delta-ferrite region, it might be expected that the transformation stresses accompanying this phase transition may result in the generation of dislocations, which, at the high pertaining temperatures, could form subgrain boundaries through polygonization. Moreover, Furuhara and Maki[11] have recently shown that sub-boundaries can also act as sites for austenite nucleation in duplex stainless steels. Therefore, it seems probable that the formation of a recovered structure in delta-ferrite could offer a means of microstructural control in the absence of plastic deformation. The aim of this work is to determine if cycling through the austenite to delta-ferrite phase transformation could lead to the generation of recovery structures. If these structures were to increase the number of sites available for austenite nucleation on cooling, the grain size of the austenite would be refined and, subsequently, the number of sites for alpha ferrite nucleation would be increased, leading to a more refined final alpha-ferrite microstructure.

II. EXPERIMENTAL

A. *High-Temperature Laser-Scanning Confocal Microscopy*

In confocal microscopy, laser light is focused by an objective lens onto the object and the reflected beam is focused onto a photo detector *via* a beam splitter. An image is built up by scanning the focused spot relative to the object, which is then stored in an imaging system for subsequent display. Through

R.J. DIPPENAAR, Director, and D.J. PHELAN, Research Fellow, are with the BHP Steel Institute, University of Wollongong, Wollongong 2500, Australia. Contact e-mail: phelan@uow.edu.au

This article is based on a presentation given in the Mills Symposium entitled "Metals, Slags, Glasses: High Temperature Properties & Phenomena," which took place at The Institute of Materials in London, England, on August 22-23, 2002.

Table I. Composition of Alloys (Mass Percent)

Steel	C	P	Mn	Si	Al	S	Cr
Al-killed	0.06	0.11	0.23	<0.005	0.04	0.014	—
Si-killed	0.06	0.10	0.40	0.29	<0.005	0.014	—
3Cr12 (typical)	0.03	0.02	1.20	0.40	—	0.005	11.36

the use of a confocal pinhole, only light incident from the focal plane is permitted to pass through to the photo detector. Hence, an extremely thin optical section is created, providing a sharp image at high resolution. Thermal radiation is also blocked by the confocal pinhole; therefore, only the polarized reflection of the high intensity laser beam reaches the imaging sensor, producing a sharp image. In these experiments, magnifications up to 1350 times were used. The laser beam, a He-Ne laser with a 632.8-nm wavelength and 0.5-μm diameter, is reflected and scanned by an acoustic optical deflector in the horizontal direction at a rate of 15.7 kHz and a galvano-mirror in the vertical direction at 60 Hz. Specimens are placed at the focal point of a gold-plated ellipsoidal cavity in an infrared furnace beneath a quartz view port. A 1.5-kw halogen lamp located at the other focal point in the cavity heats the specimen by radiation. The specimen and lamp chambers are separated by quartz glass so that the atmosphere of the specimen chamber can be controlled and the lamp air-cooled.

B. *Generation of Sub-Boundaries in Delta-Ferrite*

The delta-to-gamma and reverse phase transition was studied in two commercial low alloy steels containing 0.06 pct carbon by mass (Table I). The samples were heated to 1400 °C (γ phase) and held for 10 minutes, before heating at a rate of 100 °C/minute to 1450 °C (δ phase). Samples were then held at this temperature. This heat treatment rendered a subgrain structure in delta-ferrite. Frames were captured from the video record of events and subjected to digital image analysis to assess sub-boundary energy.

In an attempt to confirm that the phase transformation from austenite to delta-ferrite generates dislocations, which subsequently recover into low-angle boundaries, a series of experiments was conducted on a steel commercially known as 3Cr12 (Table I). A two-phase region, austenite plus delta-ferrite, exists between 1000 °C and 1150 °C in this steel. Soaking at 1400 °C for 10 minutes allowed sufficient time for large stable delta-ferrite grains to form. The sample was then cooled at 100 °C/min to 1100 °C (within the two-phase region), and sufficient time allowed for the phases to reach equilibrium. The sample was then reheated to 1400 °C while the transformation of austenite to delta-ferrite was continuously observed and the development of the microstructure recorded.

C. *Thermal Cycling through the Delta/Gamma Phase Transition*

To test whether a thermal cycle through the delta-ferrite to austenite phase fields could influence austenite decomposition, the following alloys and temperature regime were selected. The low-carbon, silicon-killed, and aluminum-killed steels listed in Table I were heated at 100 °C/min to 1450 °C and held for 10 minutes so that large stable grains of delta-ferrite were obtained. The specimens were then cycled between 1450 °C and 1350 °C, the single-phase regions of delta-ferrite and austenite, respectively, at a heating and cooling rate of 300 °C/minute. The hold time at 1450 °C and 1350 °C for the silicon-killed steel was chosen to be 0, 10, 20, 30, and 60 seconds, and for the aluminium-killed steel, 10, 25, and 40 seconds. All samples were then cooled at 100 °C/min to 700 °C, held until austenite decomposition was complete, and finally cooled to room temperature.

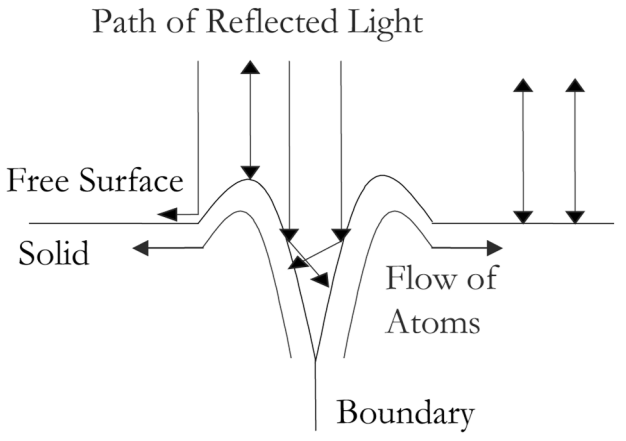

Fig. 1—Schematic representation of thermal grooving.

III. RESULTS

A. *Interpretation of LSCM Observations*

It is important to reflect upon the interpretation of *in-situ* observations made in the LSCM. The volume change accompanying a phase transformation leads to a raising or lowering of the specimen surface, locally associated with the moving interface, and this behavior leads to a change in contrast. Therefore, thermal cycling leading to repeated transformations will result in roughening of the surface to the point where the image becomes diffuse. On the other hand, surface diffusion acts to smooth the surface, especially at high temperature.

Where boundaries intersect the free surface, a groove forms as a result of diffusion of atoms from the line defect to the surface, resulting in a profile such as that presented schematically in Figure 1. The existence of such a "V" groove alters the optical path of the reflected light, and some reflected rays are scattered, leading to the development of contrast. The formation of ridges on the free surface where line defects or other interfaces intersect the surface is a result of diffusion along the interface to the free surface being faster than diffusion away from the ridged area along the surface.[12]

A ridge such as that shown in Figure 1 is likely to form whenever grain or phase boundaries intersect the free surface; the appearance of all such boundaries in laser-scanning confocal microscopy (LSCM) should be similar: a dark line boarded by areas of light contrast. A finite

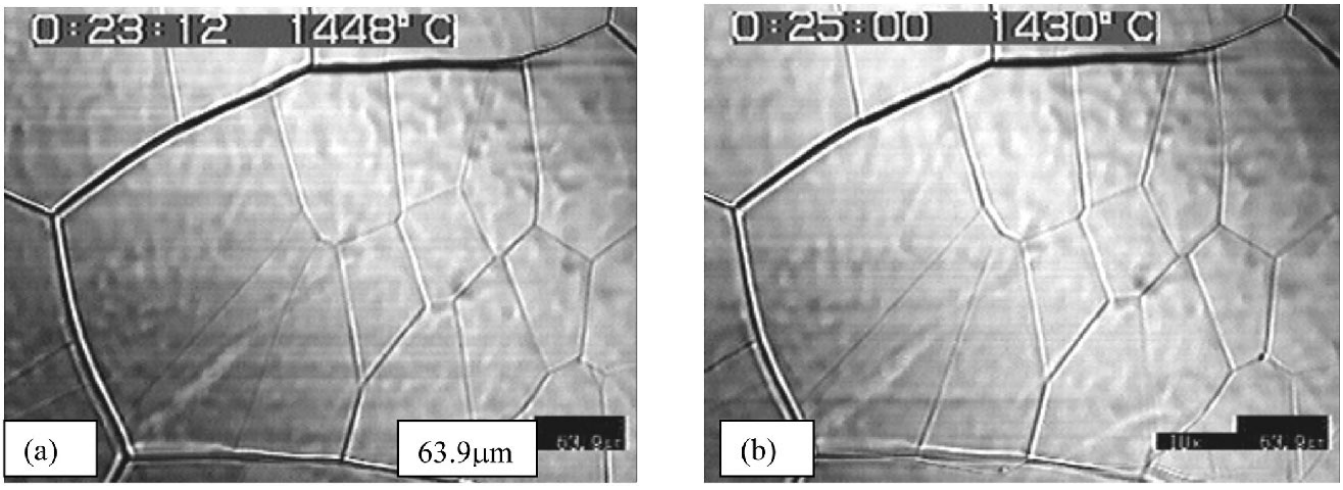

Fig. 2—*(a)* and *(b)* Delta-ferrite sub-boundaries in Si-killed steel with time.

time is required for thermal etching to form a groove, and therefore, rapidly moving boundaries are difficult to detect. The appearance in the LSCM of a moving grain boundary is very similar to that of a moving interphase boundary, and it is therefore very important to be able to distinguish between grain growth and interphase boundary movement. Consequently, if sufficient time is allowed for grain growth to cease before a phase transformation occurs, this ambiguity is eliminated and the course of events can be interpreted with confidence.

B. *Subgrain Structures in Delta-Ferrite*

A microstructure typical of the plain carbon steels shown in Table I, following heating into the delta-ferrite single-phase region, is presented in Figure 2. A fine network of sub-boundaries is observed within delta-ferrite grains. Delta-ferrite grain boundaries are high-angle interfaces and develop a pronounced thermal groove, dark black lines, and triple points of 120 deg. Sub-boundaries, on the other hand, are low-energy boundaries; therefore, they do not develop a substantial thermal groove and appear as faint lines contained within the delta-ferrite grains. Additionally, where they intersect the heavily grooved delta-ferrite grain boundaries, 120 deg triple points are not formed due to the lower energy of the sub-boundaries. The substructure is stable. The microstructure in Figure 2 was recorded over a period of 2 minutes, and, during this time, very little change was detected in the microstructure.

C. *Estimation of Sub-Boundary Energy*

To estimate the subgrain boundary energy, force balance calculations were conducted on the triple points of delta-ferrite grain boundaries and sub-boundaries. The triple points selected for measurement were restricted to those sufficiently spaced from adjacent triple points to eliminate interactions that could effect the equilibrium shape. The delta-ferrite grain boundary energy was taken as 0.471 J/m^2 (Yin *et al.*[13]). The energy balance expressed in Eq. [1] calculates the sub-boundary energy, and the values thus determined have been recorded in Table II. Although there is considerable variation in the calculated sub-boundary energies, the sub-boundary energy is substantially lower than the grain boundary energy, varying between 7 and 36 pct that of a delta-ferrite grain boundary.

Table II. Calculated Range of Sub-Boundary Energies

Steel	Minimum J/m^2	Maximum J/m^2	*n*
Al killed	0.051	0.17	15
Si killed	0.035	0.145	27

$$\sigma_{SB} = 2\sigma_{GB}\cos\left(\frac{\theta}{2}\right) \quad [1]$$

D. *Sub-Boundary Formation in Type 3Cr12 Stainless Steel*

The initial transformation from delta-ferrite to austenite on cooling a type 3Cr12 stainless steel into the two-phase delta-plus-gamma field at 1100 °C occurred predominantly along the delta-ferrite grain boundaries, with a rim of austenite covering the boundaries. However, in some instances, plates of austenite grew into the matrix of the delta-ferrite grains. Figure 3(a) shows austenite formation on delta-ferrite grain boundaries and also austenite plates that have grown into the delta matrix. On reheating to 1400 °C, within the delta-ferrite single-phase region, the austenite reverts back to delta-ferrite, as shown in Figure 3(b). A network of sub-boundaries forms only in positions where plates of austenite were present at 1100 °C. The tip of the austenite plate, expected to be associated with a stress concentration, exhibits multiple sub-boundaries running from that point into the matrix of the delta-ferrite grain. These observations provide convincing experimental evidence, albeit indirect, that the transformation from austenite to delta-ferrite does generate sufficient numbers of dislocations for recovery to be thermodynamically beneficial for the formation of low-angle boundaries (sub-boundaries).

E. *Influence of Thermal Cycling through the Delta/Gamma Phase Transition on Austenite Decomposition in Low-Carbon Steel*

Thermal cycling through the delta-to-gamma phase transition leads to surface roughening to the extent that the

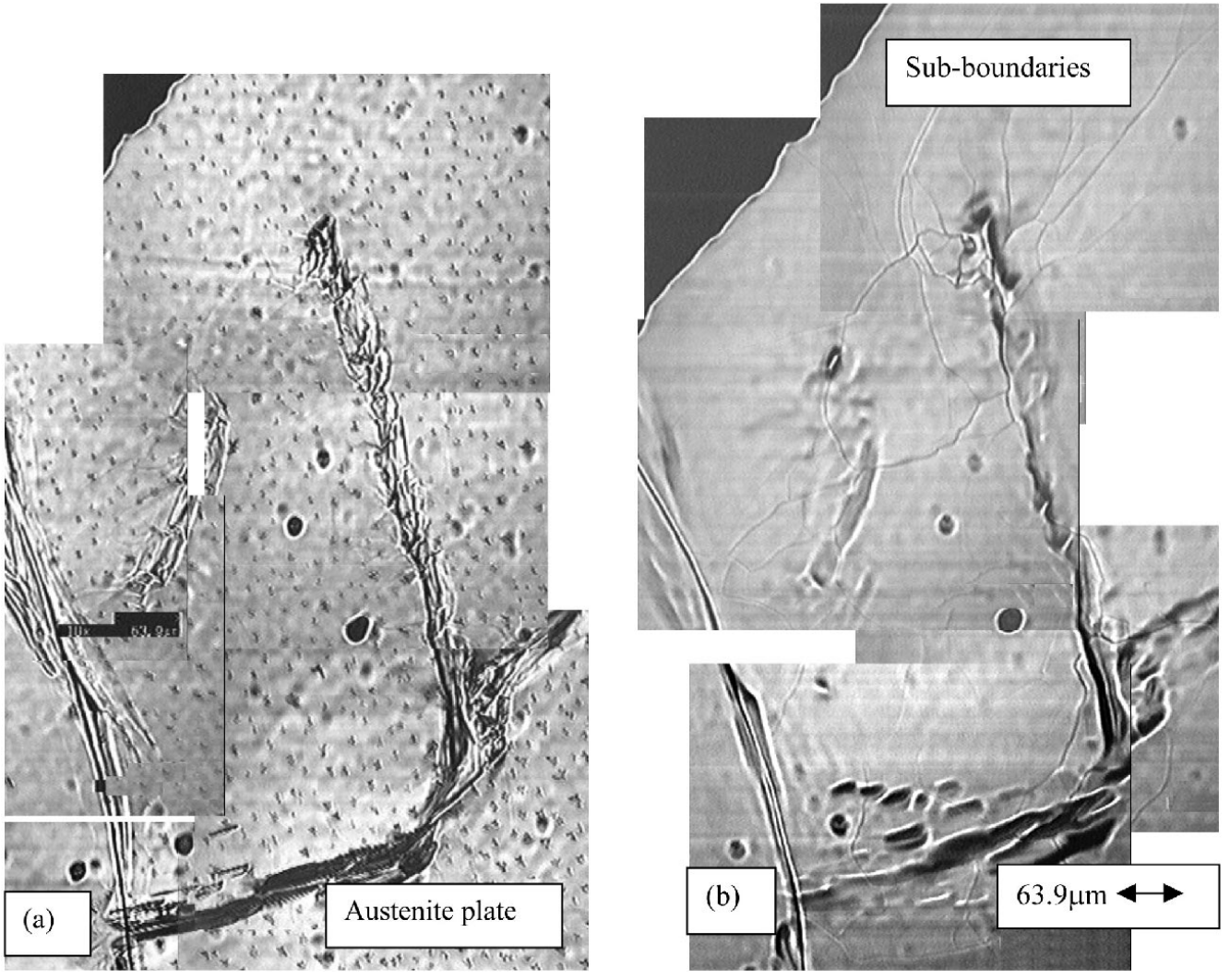

image becomes diffuse and, hence, clear LSCM micrographs could not be obtained in the thermal cycling experiments. Therefore, optical microscopy was used to characterize the microstructure following austenite decomposition, although the thermal cycling was done in the laser microscope. Following the thermal cycles, samples were mounted in bakelite, polished, etched in Nital, and the microstructure assessed by optical microscopy. Thermal cycling experiments led to a change in the microstructural development accompanying austenite decomposition. Micrographs representative of the observed changes are presented in Figure 4, taken from experiments with soak times of 0, 20, and 60 seconds for the silicon killed steel.

The microstructure following the zero soak time cycle is characterized by large, blocky structures. Widmanstätten ferrite predominates over allotriomorph ferrite (Figure 4(a)). No pearlite is present, and excess carbon has been rejected as inter- and intraplate carbides. The microstructure obtained by soaking times of 20 seconds at 1350 °C and 1450 °C is presented in Figure 4(b). The structure is comprised of polygonal ferrite and pearlite with a greatly reduced proportion of Widmanstätten ferrite. The microstructure is distinctly different from that shown in frame (a). Considering that the only variable changed was the soak time at 1350 °C and 1450 °C, the formation of the microstructure observed in Figure 4(b) cannot be explained unless the austenite grain size is smaller than that of Figure 4(a). This observation provides evidence in support of the premise that the development of a delta-ferrite recovery structure leads to the refinement of the austenite grain size when delta-ferrite transforms to austenite. The microstructure obtained by soak times of 60 seconds at 1350 °C and 1450 °C (Figure 4(c)) is characterized by large colonies of Widmanstätten ferrite; a small amount of pearlite is present but inter- and intra-granular carbides dominate. Some polygonal ferrite grains are observed. This microstructure is again distinctly different from those shown in Figures 4(a) and (b).

The measured volume fraction of Widmanstätten and polygonal ferrite/pearlite components in each microstructure is shown in Table III. The Vickers hardness of the five samples was measured with a load of 10 kg. The hard-

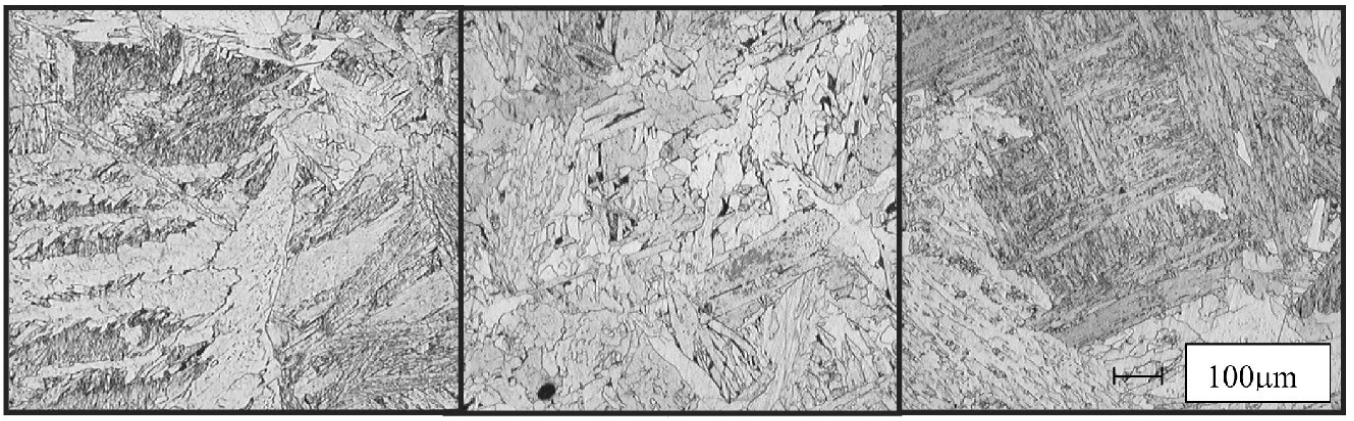

Fig. 4—Ambient optical micrographs of final microstructures (hold time of *(a)* 0 s, *(b)* 20 s, and *(c)* 60 s, silicon-killed steel).

Table III. Volume Percentage of Decomposition Products and Vickers Hardness (VH) (Si-Killed)

Soak Time (s)	Widmanstätten (Vol Pct)	Polygonal ferrite/Pearlite (Vol Pct)	Hardness	
			Average VH 10	Standard Deviation
0	99	1	123.4	3.497
10	92	8	121.4	3.851
20	6	94	114.0	2.732
30	34	64	118.4	4.177
60	95	5	120.1	3.341

Table IV. Vickers Hardness (VH) Measurements of Al-Killed Steel (5-kg Load)

Soak Time (s)	Average VH	*n*	Standard Deviation	F-Test (cf. 25 s)
10	96.3	9	5.82	0.0019
25	95.4	10	1.78	—
40	102.4	10	8.01	0.0003

ness and standard deviations are tabulated in Table III. Despite the large standard deviations in the measured hardness numbers, the average measured hardness is statistically different. This analysis provides a quantifiable measure to indicate that not only is the thermal treatment modifying the microstructure, but also the mechanical properties. This experimental evidence clearly shows that the final microstructure following decomposition of austenite below 900 °C is influenced by thermal cycling through the delta/gamma phase transition occurring at a temperature of approximately 1400 °C.

The hardness results tabulated in Table IV for the aluminum-killed steel are more ambiguous than those for the silicon-killed steel. Statistically, the mean hardness values cannot be said to be different with a high confidence. However, on the basis of variability in the samples, as determined by the F-test, there is a greater than 99 pct confidence that there is a statistical difference between a 25-s soak time and soak times of 10 and 40 seconds.

IV. DISCUSSION

Although LSCM seems eminently capable of being used as a technique to study events occurring at high temperature, care has to be taken in the interpretation of observations made. Phelan[14] has recently shown that there exists a nexus between phase transformations observed on the free surface in LSCM and events occurring in the bulk. On the other hand, grain boundary movement and precipitation of nonmetallic inclusions are influenced by the nature of the free surface, and observations in the LSCM do not necessarily correlate with bulk behavior.

The phenomenon of delta-ferrite sub-boundaries is illustrative of these issues. Sub-boundaries observed on the free surface do possess a bulk presence; this observation can be surmised by the fact that they are stable over a period of minutes. At the high temperatures involved, the high rate of surface diffusion quickly acts to smooth away grooves not possessing a bulk presence, for example, a

groove left behind following grain growth. On the other hand, the free surface characteristics do influence our observation and interpretation of events, demonstrated by the relative difference in appearance of the sub-boundaries in the aluminum- and silicon-killed steels. This observation is specifically interesting because Yin *et al*.,[13] who studied the delta-to-gamma transformation in aluminum-killed steels *in-situ* using LSCM, did not report the presence of such delta-ferrite sub-boundaries. It is possible that they may not have observed these sub-boundaries because they are very faint and difficult to resolve in aluminum-killed steel.

It is proposed that these subgrains form in the delta-ferrite matrix by the rearrangement of dislocation networks by a process of polygonization. It is also proposed that these dislocations are generated by a combination of transformation stresses and the difference in thermal expansion coefficients of the delta and gamma phases. It is clearly important to seek experimental evidence in support of the premise that transformation stresses induce dislocation generation, which, in turn, results in polygonization. It is specifically important to prove that such a dislocation structure can form on heating austenite into the delta-ferrite phase field. It is not possible to observe dislocations in the LSCM, or in transmission electron microscopy at the high pertaining temperature. The experiments conducted on the 3Cr12 steel provide compelling evidence for the role of the austenite to delta-ferrite phase transformation in sub-boundary formation. In Figure 3, the austenite phase has formed predominantly along the delta-ferrite grain boundaries, but also as a plate into the bulk of the grain. It is expected that a significant stress concentration would be present at the tip of such a plate, and it is thought that this stress concentration, combined with the transformation stresses, may generate dislocations on reheating into the delta-phase field. Should sufficient dislocations form, polygonization might lead to the formation of sub-boundaries; this explanation appears to be what has happened in the specimen shown in Figure 3(b). Subgrain boundaries have formed in the area around the tip of the plate where the highest stress concentration is expected, and also where the austenite plate was located. Although this observation was made in a ferritic stainless steel, it seems reasonable to expect that dislocation networks may also form during the transformation of austenite to delta ferrite in plain carbon steel.

The authors have also proposed that the final microstructure in low-carbon steel, resulting from the decomposition of austenite, may be influenced by the existence of a subgrain structure in the delta-ferrite phase. Convincing experimental evidence was provided in support of the premise that repeated cycling through the delta/gamma phase transition would develop a well-defined subgrain structure in the delta phase. This substructure provides additional austenite nucleation sites, which leads to a refinement of the gamma structure, which, in turn, leads to a modified ferrite microstructure on decomposition of the austenite. This result is an exciting prospect because it means that the formation of a substructure in delta-ferrite could, in principle, provide a means of microstructural modification and control of the final product in the absence of mechanical work. Such a procedure would have specific relevance to the strip casting of low-carbon steels where control of microstructural development through thermomechanical processing is not possible. Additionally, because the strip-cast product is thin steel sheet, it can be heated and cooled very rapidly, and hence, thermal cycling can be done more easily than with conventionally continuously cast steel.

The development of sub-boundaries through recovery does not occur instantaneously but as a function of time. During this period, the delta-ferrite grains may grow by the normal mechanism of grain growth and hence there are two competing processes at play: subgrain formation and delta-ferrite grain growth. A well-developed subgrain structure will refine the ensuing austenite grain size while delta-ferrite grain growth will have the opposite effect. The kinetics of neither process has been adequately studied in delta-ferrite and, hence, only qualitative conclusions can be drawn. However, it is reasonable to assume that these two competing processes will result in an initial refinement of the microstructure as sub-boundaries develop, but with time, delta-ferrite grain growth would dominate, reducing the number of nucleation sites available for austenite formation, not only through a reduction in the grain boundary area, but also through sweeping up the sub-boundaries themselves. This proposed sequence of events could explain the initial refinement followed by coarsening at longer soak times of the microstructures shown in Figure 4. In the absence of quantified kinetic data on subgrain formation and delta-ferrite grain growth, the proposed sequence of events provides a plausible explanation for the observed microstructural changes.

V. CONCLUSIONS

1. Sub-boundaries have been observed in the delta-ferrite phase of low-carbon steels.
2. It is proposed that dislocations are generated by the strains associated with the austenite to delta-ferrite transformation on heating. These dislocations eventually form sub-boundaries through the process of polygonization.
3. Experiments conducted with a ferritic stainless steel provided evidence in support of this proposed mechanism.
4. Experimental evidence was found for the proposition that the sub-boundary structure in delta-ferrite can play a role in modifying austenite decomposition products.
5. The ability to control microstructural development without recourse to thermomechanical processing could, in principle, provide a novel means of microstructural modification and control, especially in near-net shape casting processing.

ACKNOWLEDGMENTS

The authors thank Mr. Mark Reid, the University of Wollongong, BHP Steel, and the Australian Research Council.

REFERENCES

1. H.I. Aaronson: *Mater. Forum*, 1999, vol. 23, pp. 1-22.
2. P.J. Clemm and J.C. Fisher: *Acta Metall*., 1955, vol. 3, pp. 70-73.

3. W. Huang and M. Hillert: *Metall. Trans. A*, 1996, vol. 27A, Feb., pp. 480-83.
4. M. Enomoto, W.F. Lange, and H.I. Aaronson: *Metall. Trans. A*, 1986, vol. 17A, pp. 1399-1407.
5. M. Ferry, M. Thomson, and P.A. Manohar: *Iron Steel Inst. Jpn*., 2002, vol. 42, pp. 86-93.
6. K. Mukunthan, L. Strezov, R. Mahapatra, and W. Blejde: *Proc. Brimacombe Memorial Symp*., Vancouver, Oct. 2000, G.A. Irons and A.W. Cramb, eds., TMS, Warrendale, PA, 2000, pp. 421-38.
7. N.P. Goss: *Trans. AIME*, 1941, vol. 145, pp. 272-80.
8. J.J. Hauser, J.M. Capenos, and B.R. Banerjee: *ASM Trans. Q*., 1961, vol. 54, pp. 514-25.
9. A.J. Baker, P.M. Kelly, and J. Nutting: *Electron Microscopy and Strength of Crystals*, University of California, Berkeley, CA, July 5-8, 1961, G. Thomas and J. Washburn, eds., Interscience Publishers, New York, 1963, pp. 899-916.
10. J. Talbot: *Recovery and Recrystallisation of Metals*, Interscience Publishers, New York, NY, 1963, pp. 269-303.
11. T. Furuhara and T. Maki: *Mater. Sci. Eng. A*, 2001, vol. 312, (1-2), pp. 145-54.
12. N. Zapsukalov and R. Dippenaar: University of Wollongong, Wollongong, private communication, 2001.
13. H. Yin, T. Emi, and H. Shibata: *Acta Mater*. 1999, vol. 47(5), pp. 1523-35.
14. D. Phelan: Ph.D. Thesis, University of Wollongong, Wollongong, 2002.